

Received 15 August 2022, accepted 27 August 2022, date of publication 29 August 2022, date of current version 6 September 2022.

Digital Object Identifier 10.1109/ACCESS.2022.3202931

RESEARCH ARTICLE

Blood Oxygen Concentration and Physiological Data Changes During Motion While Wearing Face Masks

HANA CHARVÁTOVÁ¹, ALEŠ PROCHÁZKA^{2,3,4}, (Life Senior Member, IEEE),
MATĚJ FRIČL², AND OLDŘICH VYŠATA⁴, (Member, IEEE)

¹Faculty of Applied Informatics, Tomas Bata University in Zlín, 760 01 Zlín, Czech Republic

²Department of Computing and Control Engineering, University of Chemistry and Technology at Prague, 160 00 Prague, Czech Republic

³Czech Institute of Informatics, Robotics and Cybernetics, Czech Technical University of Prague, 160 00 Prague, Czech Republic

⁴Department of Neurology, Faculty of Medicine, Charles University at Hradec Králové, 500 05 Hradec Králové, Czech Republic

Corresponding author: Hana Charvátová (hcharvatova@email.cz)

This work was supported in part by the Development of Advanced Computational Algorithms for Evaluating Post-Surgery Rehabilitation under Grant LTAIN19007; and in part by the National Sustainability Program Project of the Ministry of Education, Youth and Sports of the Czech Republic under Grant LO1303 (MSMT-7778/2014).

This work involved human subjects or animals in its research. Approval of all ethical and experimental procedures and protocols was granted by the Ethics committee of the Neurological Center at Rychnov n. Kn., Czech Republic.

ABSTRACT The study of physiological changes recorded by wearable devices during physical exercises belongs to very important research topics in neurology for the detection of motion disorders or monitoring of the fitness level during sports activities. This paper contributes to this area with studies of the effect of face masks and respirators on blood oxygen concentration, breathing frequency, and the heart rate changes. Experimental data sets include 296 segments of their total length of 60 hours, recorded on a home exercise bike under different motion conditions. Wearable instruments with oximetric, heart rate, accelerometric, and thermal camera sensors were used to fill the own database of signals recorded with selected sampling frequencies. The proposed methodology includes fundamental signal and image processing methods for signal analysis and machine learning tools for labeling image components and detecting facial temperature changes. Results show the minimal effect of mask wearing on blood oxygen concentration but its substantial influence on the breathing frequency and the heart rate. The use of a respirator substantially increased the respiratory rate for the given set of experiments under the load. This indicates how wearable sensors, computational intelligence, and machine learning can be used for motion monitoring and data analysis of signals recorded in different conditions.

INDEX TERMS Motion monitoring, wearable sensors, blood oxygen concentration, breathing analysis, computational intelligence, machine learning, classification.

I. INTRODUCTION

The analysis of motion patterns acquired under different conditions and studies of physiological functions belongs to very important research topics with significant applications in neurology, rehabilitation, and monitoring of sport activities [1], [2], [3], [4]. Physiological signals include the heart rate, blood

oxygen concentration [5], [6], breathing rate, acceleration, and positioning records using camera systems and satellite navigation [7] in many cases.

There are specific studies that are devoted to the influence of surgical mouthpieces and face masks [8], [9] on dyspnoea and cardiorespiratory parameters during different ways of movement. Some results show that face masks have a minimal impact during short exercise tests [10], [11] while other papers [12] point to a reduction of the blood oxygen

The associate editor coordinating the review of this manuscript and approving it for publication was Filbert Juwono¹.

concentration, an increase in the frequency of the heartbeat, and a sensation of shortness of breath.

Measurement techniques include the use of wearable sensors [13], [14], thermal and depth cameras, oximeters, and heart rate sensors to acquire specific body signals and video-records [6], [15], [16]. The home exercise bike forms a very useful device for recording these data under selected loads and for performing sets of experiments [17], [18]. The results can be further verified during cycling in real conditions [19].

Different microelectromechanical sensor units (MEMS), accelerometers, smartphones, and smartwatches include further sensors that can be used for biometric data acquisition. Associated problems include the selection of the sampling frequency and the choice of communication links for transmitting the data.

Appropriate computational methods of signal and image processing together with machine learning tools are then applied to extract the desired information. These computational tools include methods of signal analysis in the time, frequency, and scale domains [20], [21], methods of digital filtering to reject noise components [22], and computational intelligence methods for extracting signal features.

The present paper is devoted to the analysis of blood oxygen concentration, heart rate estimation, breathing frequency evaluation, and processing of accelerometric signals recorded during exercises on a home exercise bike. Specific adaptive methods are proposed for detecting breathing frequency using infrared thermography and video records of the facial area [15], [23], [24]. The methodology proposed for the analysis of these multimodal signals [25] includes their time-synchronisation, detection of specific image components for breathing rate estimation, and the analysis of physiological signals during different body loads.

II. METHODS

A. DATA ACQUISITION

All experiments were done on a home exercise bike with data acquired during different motion patterns. Sensors included a pulse oximeter for blood concentration and heart rate recording, thermal camera to follow breathing, and an accelerometer inside a mobile phone to analyze motion data.

The global analysis [26] of blood oxygen concentration, heart rate changes, and breathing analysis were done during experiments of 16 individuals (11 males and 5 females between 24 and 48 years old) on a home exercise bike. Physiological data of separate segments were recorded during 64 load and 64 rest periods that were 9 and 6 minutes long, respectively. Half of experiments were done with the uncovered face and the second one with the FFP2 respirator. The whole study includes 1920 minutes of recorded signals.

The more detail analysis of changes of blood oxygen concentration, heart rate, and breathing frequency were done for a selected individual during (i) seven experiments without any

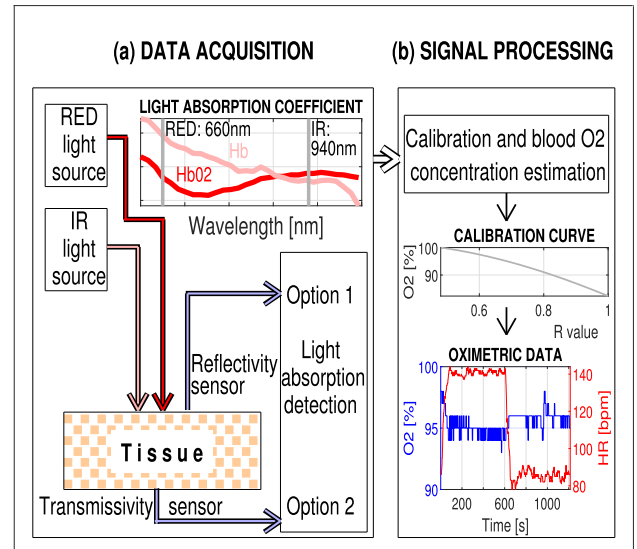


FIGURE 1. Principle of the blood oxygen concentration measurement with the reflectivity or transmissivity sensor, presenting (a) the use of two light sources (RED and infrared IR) for the tissue illumination with the light absorption detection and (b) signal processing for system calibration and for the estimation of the heart rate and blood oxygen concentration.

cover on the face, (ii) seven experiments with a three-layer face mask, and (iii) seven experiments with a five-layer FFP2 respirator to study the effect of a face cover on physiological functions. Each experiment was 80 minutes long and included four observations. Each of them was composed of one segment recorded with a load and the following one acquired during resting, each of them 10 minutes long. The whole study is based on 168 segments with data recorded during 1680 minutes.

The blood oxygen concentration and the heart rate measurement were recorded by a pulse oximeter [27], [28], [29], [30], [31] with the reflectivity or transmissivity sensor and the sampling frequency of 1 Hz. The sensor for the blood oxygen concentration (Fig. 1) is a non-invasive device with two light sources that include red and infrared light of 650 nm and 940 nm, respectively. The tissue is illuminated and another sensor (light detector) receives either reflected or transmitted light that has not been absorbed or scattered. The sensor uses a non-invasive principle, photoplethysmography (PPT), to detect blood volumetric changes in the peripheral circulation. The observed values with their timestamps were time-synchronised with the mobile phone and transmitted with their comma separated values (CSV) through wireless communication links.

Changes of breathing rate were followed by an infrared thermal camera in front of the individual. The time evolution of temperature changes was acquired in the facial area of all video recordings. The video record of the thermal camera acquired for each experiment was transformed into a sequence of images with a resolution of 240 by 320 elements and frame rate of 10 fps, which makes for more than one million images available for data analysis. Each image was

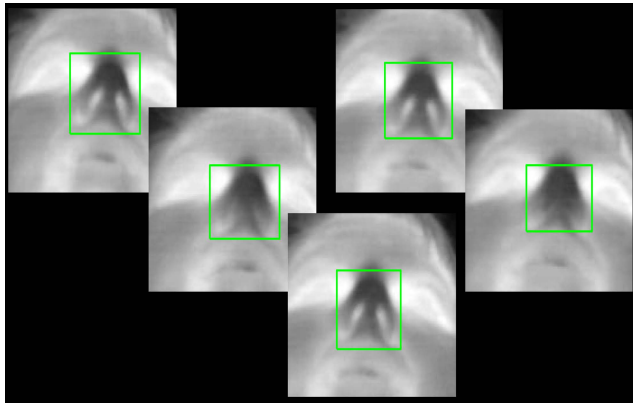


FIGURE 2. The sequence of subsequent infrared thermal images recorded without the mask with regions of interests around the nose.

then reduced by 20% on each side to optimise the processing time. Further reduction was achieved by a change of frame rate to 2 Hz for analysis of images with uncovered face owing to the sampling theorem and maximum breathing rate of 0.7 Hz for these experiments. Temperature changes caused by breathing were then detected either inside the nose or on the face mask and respirator. Fig. 2 presents a selected set of thermal images with regions of interest (ROI) acquired without any face cover that includes the nose area for the time evolution of thermal changes and evaluation of the breathing frequency. The processing of the thermal images with the face mask and respirator is easier, as the region of interest is much larger. Fig. 3 presents a selected thermal image matrix with the associated thermo bar and the time evolution of the mean temperature values in the region with its highest changes. The association of image shades with temperatures was performed by a neural network model [15] as well as the detection of the temperature inside each thermo frame.

Accelerometric signals were recorded by the sensor of the mobile phone located in the spine area of the body, a position which has higher discriminative abilities in comparison to other positions [3], [32], [33]. The sampling frequency of the mobile Matlab and the phone sensor was 100 Hz during all cycling experiments. A sample record of these data during the load and the rest periods is presented in Fig. 4.

These procedures involving human participants were in accordance with the ethical standards of the Institutional research committee and with the 1964 Helsinki Declaration and its later amendments.

B. SIGNAL PROCESSING

The mathematical methods of the data processing are closely related to the properties of the sensors used for their acquisition. But in general, de-noising, analysis in the selected transform domain, and the extraction of features form common problems.

Oximeters are used for the measurement of the oxygen saturation, defined as the amount of oxygen dissolved in the blood. A simple diagram of this system is presented in

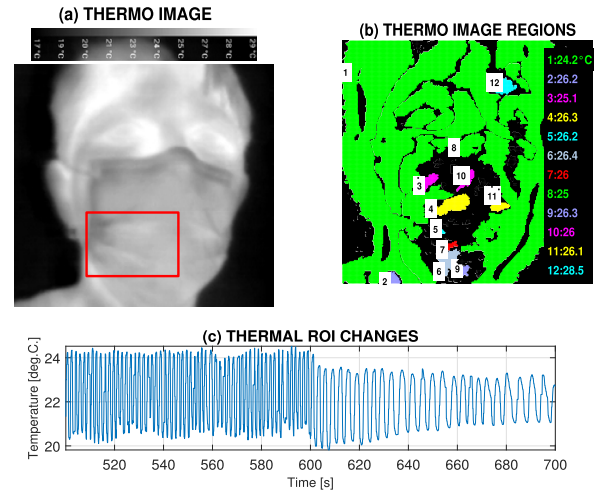


FIGURE 3. Main steps of thermal video sets including (i) a selected thermal image matrix with the associated thermo bar that associates shade levels and temperatures, (b) thermal image areas with highest temperature gradients, and (c) the time evolution of the mean temperatures in the region with their highest changes during cycling experiments performed with different loads.

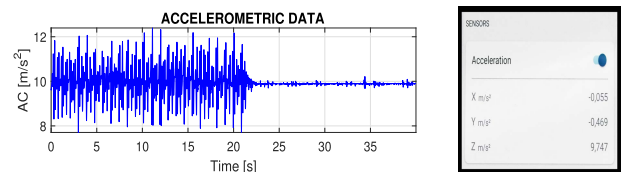


FIGURE 4. Accelerometric signals recorded on the home exercise bike during the load/rest periods and the mobile MATLAB screen showing separate data values.

Fig. 1. Oxygenated hemoglobin (HbO₂) has a higher absorption for infrared light while deoxygenated hemoglobin (Hb) has a higher absorption for red light. The extinction coefficient has two components: the DC_{xx} component, representing time-independent tissue absorption, and the AC_{xx} component, related to the pulsative arterial blood that has its maximum $AC_{max_{xx}}$ and minimum $AC_{min_{xx}}$ for the specific wavelength xx . This fact is used for the evaluation of the absorption coefficient [28] defined by the following relation using values for the red ($xx = 650$ nm) and infrared ($xx = 940$ nm) light:

$$R = \frac{(AC_{max_{660}} - AC_{min_{660}})/DC_{660}}{(AC_{max_{940}} - AC_{min_{940}})/DC_{940}} \quad (1)$$

The blood oxygen concentration is related to this relation by the calibration empirical formula. A typical one is defined by the following relation [28]:

$$SP = 10.0002 * R^3 - 52.887 * R^2 + 26.871 * R + 98.283 \quad (2)$$

The principle of the detection of the ROI of the nose area in infrared thermal images used for estimating the breathing frequency for an uncovered face is presented in Fig. 2 showing results of automatic ROI labeling. The algorithmic solution is based on the semantic segmentation [34], [35] that can predict

the semantic category of each image pixel from a given set of labels using deep learning. Processing of these records in the Matlab environment includes:

- Manual detection of ROIs for a small number of images, training of the model, and evaluation of parameters for automatic detection of these labeled areas [36];
- The implementation of the proposed model in an automatic image labeler and its application to detecting the bounding boxes of the ROIs for the whole extensive set of facial images;
- Evaluation of the mean shade level in each bounding box during the different activity loads.

Facial images with a covered face were processed by the proposed adaptive algorithm [15] that detected the region with the highest changes of temperature. In all cases, the mean values of the shade in the associated bounding box were evaluated. The association of image shades with temperatures was then performed by the neural network model of [15] to detect the mean temperatures inside each thermo frame.

The accelerometric components $ax_q(n)$, $ay_q(n)$, and $az_q(n)$ recorded in three directions were then used to evaluate its modulus:

$$a_q(n) = \sqrt{ax_q(n)^2 + ay_q(n)^2 + az_q(n)^2} \quad (3)$$

for all values of $n = 0, 1, 2, \dots, N - 1$ in each segment $q = 1, 2, \dots, Q$ composed of N values to evaluate values invariant to the rotation of the sensor.

The time series $\{x(n)\}_{n=0}^{N-1}$ of temperature values and acceleration in each segment were then smoothed by the selected finite impulse response filter (FIR) of order $M = 60$ defined by the relation:

$$y(n) = \sum_{k=0}^{M-1} b(k) x(n - k) \quad (4)$$

with the selected cutoff frequency to evaluate a new sequence $\{y(n)\}_{n=0}^{N-1}$ for all values of $n = 0, 1, 2, \dots, N - 1$ and for filter coefficients $\{b(k)\}_{k=0}^{M-1}$.

The breathing frequency was then evaluated from the spectrum of this sequence estimated by the short-time Fourier transform (STFT) of each window L samples long as follows:

$$Y_w(k) = \sum_{n \in S_w} y(n) \exp(-j k n 2 \pi / L) \quad (5)$$

for the sequence of signal values in each (overlapping) analysing STFT window w of the slected sequent q with their indices in the set S_w .

The accelerometric data were processed in the spectral domain as well. The relative energy E_q in the frequency band $\langle fc_1, fc_2 \rangle$ was evaluated by

$$E_q = \frac{\sum_{k \in \Phi} |Y_q(k)|^2}{\sum_{k=0}^{N/2} |Y_q(k)|^2}, \quad (6)$$

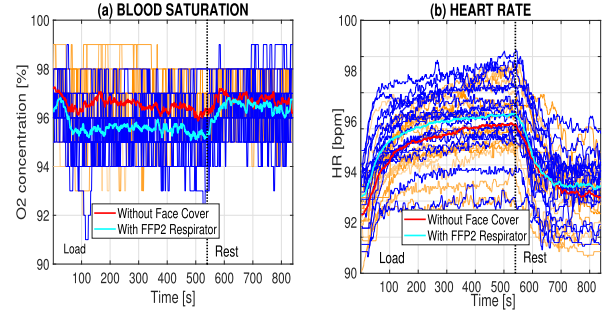


FIGURE 5. The evolution of (a) the blood O2 concentration and (b) the heart rate of 16 individuals during the load and rest periods for experiments without any face cover and with the FFP2 respirator.

where Φ is the set of indices for the frequency components $f_k \in \langle fc_1, fc_2 \rangle$ for each segment q .

III. RESULTS

All signals acquired during experiments were time-synchronised, preprocessed by digital filtering, and segmented in the computational environment of MATLAB 2022a.

Results of the global analysis of experiments on the home exercise bike are presented in Fig. 5. Changes of the blood O2 concentration and the heart rate of 16 individuals during the load and rest periods with mean values and experiments without any face cover and with the FFP2 respirator are very close. Table 1 presents mean values and standard deviations of the heart rate and breathing frequencies for the subset of males, females, and the whole set of 16 individuals for different types of experiments. Physiological features are slightly better for experiments without the face cover but these changes are negligible.

TABLE 1. Mean values (Mean) and standard deviations (STD) of the heart rate and breathing frequencies for the subset of males, females, and the whole set of 16 individuals for experiments without any face cover (NoCover) and with the FFP2 respirators (Resp).

Set	Heart Rate [bpm]		Breathing Freq. [Hz]	
	NoCover	Resp	NoCover	Resp
Male	Mean	137.3	0.327	0.388
	STD	19.5	0.039	0.066
Female	Mean	160.5	0.314	0.422
	STD	14.41	0.087	0.111
All	Mean	144.6	0.320	0.400
	STD	20.8	0.056	0.080

More detail analysis of a selected individual in Fig. 6 presents the evolution of the blood oxygen concentration and the heart rate during the load and rest periods with the face covered by a respirator. In all cases, the mean value of the blood oxygen concentration is slightly higher during the rest period than during the load period. More detailed results both for a face mask and a respirator are presented in Table 2.

Figure 7 presents the evolution of the temperature in the nose area as well as the evolution of the breathing frequency,

TABLE 2. Specification of segments for the mean blood O₂ concentration, mean heart rate, breathing frequency, and acceleration in the selected frequency range for load (L) and rest (R) segments with no face cover (Face), with a face mask (Mask) and with a respirator (Resp) evaluated during the second half of each segment.

Class	No	O ₂ concentration		Heart Rate		Breathing Frequency		Acceleration	
		Mean [%]	STD	Mean [bpm]	STD	Mean [Hz]	STD	Mean [%]	STD
L-Face	18	95.54	1.25	155.4	0.27	0.34	0.020	45.2	5.04
R-Face	18	95.98	0.71	92.4	0.72	0.19	0.006	5.5	0.91
L-Mask	24	94.48	0.83	152.7	0.29	0.63	0.031	44.3	4.00
R-Mask	24	95.71	0.54	90.7	1.87	0.27	0.020	3.3	0.88
L-Resp	24	94.81	1.18	162.1	0.25	0.65	0.024	45.9	4.63
R-Resp	24	95.70	0.48	101.9	0.80	0.20	0.015	2.1	1.07x

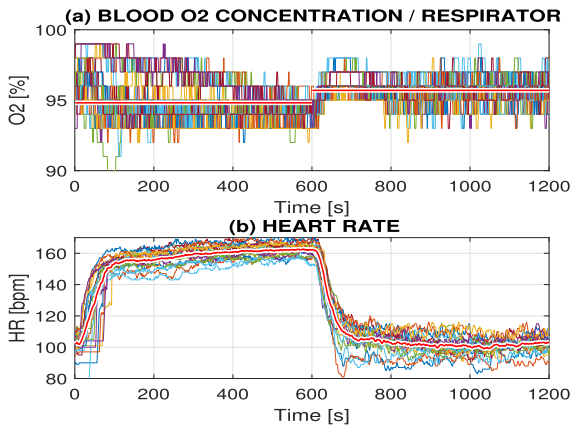


FIGURE 6. The evolution of mean physiological characteristics during the load and rest periods on the home exercise bike presenting (a) the blood O₂ concentration and (b) the heart rate.

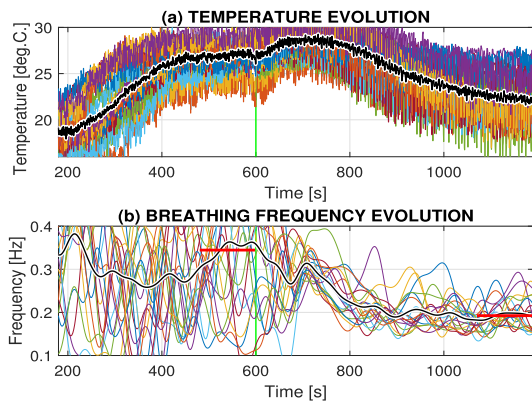


FIGURE 7. Facial thermo data processing presenting (a) the temperature evolution in the nose area and (b) the breathing frequency evolution for the load and rest regions evaluated for 18 segments with their mean values acquired on the home exercise bike without any cover of the face.

both for periods under load and resting, evaluated for 36 segments with their mean values acquired on the home exercise bike without any face cover. The frame rate of 2 Hz was sufficient in this case since the mean frequency change was 0.34 Hz (20.7 bpm) during the last minute of the exercise in the load segment and 0.19 Hz (11.6 bpm) in the last minute of the rest segment. Figure 8 presents facial thermo data processing recorded with a face cover, presenting the evolution of the

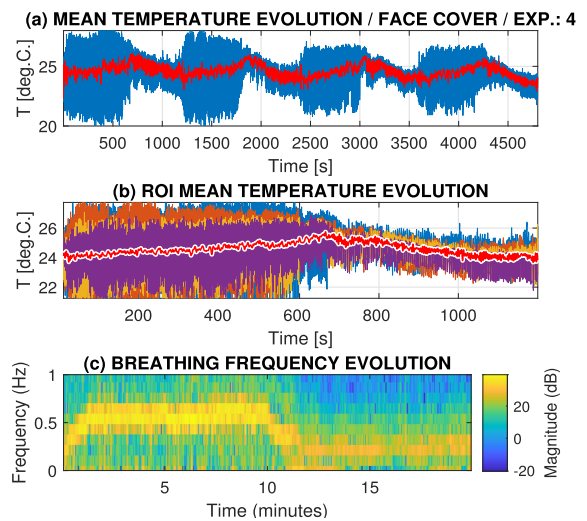


FIGURE 8. Facial thermo data processing presenting (a) the mean temperature evolution for 4 subsequent tests, (b) the mean temperature evolution of 4 tests, and (c) the mean breathing frequency evolution for the load and rest regimes and the face cover.

mean temperature for 4 subsequent observations of a selected experiment, the evolution of the mean temperature and that of the mean breathing frequency, both for the load and rest periods. A comparison of the breathing rate for the covered and uncovered face is presented in Table 2. The breathing rate for the load segment is 89% higher than the experiment with the respirator in comparison with that without any face cover.

Figure 9 presents the time and frequency evolution of accelerometric data for four load and four rest periods acquired on the home exercise bike for a selected experiment and the respirator use. Spectral components for load and rest periods are presented in Figs. 9(a) and (b), respectively, with their different layouts. More detailed statistics are presented in Table 2 with a comparison of the results obtained for the covered and uncovered face. The relative percentage of energy in the frequency range of 2–8 Hz is evaluated as a feature of the motion pattern and can be used for the subsequent classification.

Three complete datasets recorded without any face cover, with a face mask, and with a respirator are stored at the IEEE DataPort (<http://iee-dataport.org/9578>) for further investigation. This repository includes also the Matlab source code and

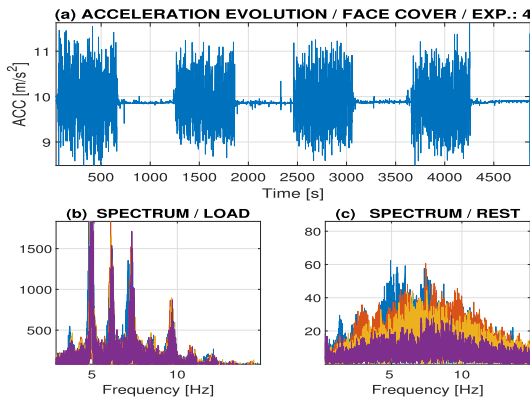


FIGURE 9. Accelerometric data presenting (a) the time evolution of accelerometry, (b,c) the frequency evolution for the load and rest regimes acquired on the home exercise bike.

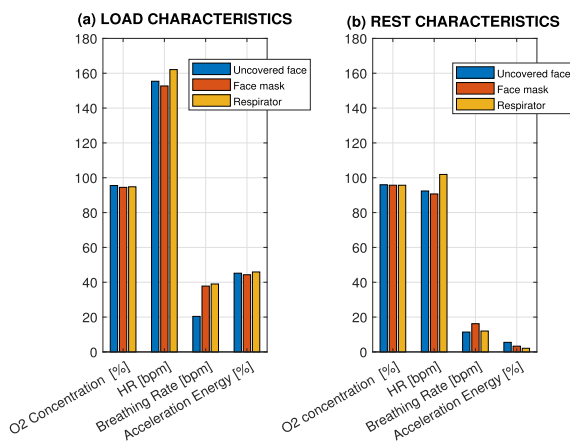


FIGURE 10. Comparison of physiological characteristics for uncovered face, face mask, and respirator use for experiments during (a) the load and (b) the rest period on the exercise bike.

data for demonstration of blood concentration, heart rate, and breathing data extraction that generate the graphical video abstract of the paper.

IV. DISCUSSION

Global experiments performed for 16 individuals and 128 segments proved nearly no effect of respirators on the blood oxygen concentration and the heart rate. The increase of the heart rate by about 3.2 % was compensated by the increase of the breathing frequency by about 25 %.

Figure 10 presents detail analysis of physiological characteristics summarised in Table 2. Mean values of specific features for segments with uncovered face, face mask and respirator are compared both for segments recorded during the load and rest in Figs. 10(a) and (b), respectively. The results of the set of experiments on the exercise bike show that the blood oxygen concentration is nearly the same for experiments with an uncovered face, with a face mask, and with a respirator. The heart rate for experiments with a respirator is higher both for load and rest experiments in comparison with the other ones. The two-sample t-test was evaluated to test the decision for the null hypothesis that blood concentration

and heart rate data in the middle of the load/rest period of signals recorded without any face cover and with either a face mask or a respirator come from independent random samples with equal means. This hypothesis was accepted at the 5 % significance level.

The breathing frequency was estimated from the temperature changes in the facial area recorded by the thermal camera. The breathing rate was higher for experiments with a face mask or respirator. This result explains the nearly unaffected concentration of the blood oxygen concentration. The mean breathing rate during the load period increased from 0.19 Hz (11.4 bpm) for the uncovered face to 0.65 Hz (39.0 bpm) with the use of a respirator which represents 89 % for the given set of experiments.

The relative motion energies evaluated from the accelerometric data are very close for all kinds of experiments. The use of this characteristic is in the subsequent classification of different kinds of motion, important in neurology and rehabilitation for monitoring and analysis of motion patterns.

V. CONCLUSION

This paper presents the use of computational methods for processing physiological data during motion on a home exercise bike with an uncovered face, with a face mask, and with a respirator, under different motion conditions. Its results show nearly no effect of the face cover on blood oxygen concentration, which is compensated for by the higher breathing rate.

These results are concordant with those of other studies that confirm the minimal impact of face masks wearing during short time periods [10], [11], [37], [38]. Latest extensive studies investigated the effect of face masks [39] while working during the long time periods of 12-h shifts for the blood saturation and heart rate. A small median decrease of blood oxygen concentration of 1 % was recorded. No significant differences between men and women or between older and younger individuals in terms of the blood oxygen concentration and heart rate were observed. The reduced oxygen saturation when wearing a mask has not yet been supported by available data [40] even though some papers [41] admit their influence without affecting heart rate.

The paper forms a contribution to hypothesis that wearing face masks and respirators during physical experiments does not statistically affect blood oxygen concentration and heart rate. More extensive data sets, complex sensor systems, and sophisticated mathematical methods should be included in further research.

REFERENCES

- [1] C. Buckley, L. Alcock, R. McArdle, R. Rehman, S. D. Din, C. Mazzà, A. Yarnall, and L. Rochester, “The role of movement analysis in diagnosing and monitoring neurodegenerative conditions: Insights from gait and postural control,” *Brain Sci.*, vol. 9, no. 2, p. 34, Feb. 2019.
- [2] O. Geman, S. Saneı, I. Chiuchisan, A. Graur, A. Prochazka, and O. Vysata, “Towards an inclusive Parkinson’s screening system,” in *Proc. 18th Int. Conf. Syst. Theory, Control Comput. (ICSTCC)*, Sinaia, Romania, Oct. 2014, pp. 475–481.
- [3] A. Prochazka, O. Dostal, P. Cejnar, H. I. Mohamed, Z. Pavelek, M. Valis, and O. Vysata, “Deep learning for accelerometric data assessment and ataxic gait monitoring,” *IEEE Trans. Neural Syst. Rehabil. Eng.*, vol. 29, pp. 360–367, 2021.

- [4] H. Charvatova, A. Prochazka, O. Vysata, C. P. Suarez-Araujo, and J. H. Smith, "Evaluation of accelerometric and cycling cadence data for motion monitoring," *IEEE Access*, vol. 9, pp. 129256–129263, 2021.
- [5] Z. Kalyuzhner, S. Agdarov, A. Bennett, Y. Beiderman, and Z. Zalevsky, "Remote photonic sensing of blood oxygen saturation via tracking of anomalies in micro-saccades patterns," *Opt. Exp.*, vol. 29, no. 3, p. 3393, 2021.
- [6] M. Nitzan, I. Nitzan, and Y. Arieli, "The various oximetric techniques used for the evaluation of blood oxygenation," *Sensors*, vol. 20, no. 17, p. 4844, Aug. 2020.
- [7] A. Procházka, S. Vaseghi, M. Yadollahi, O. Ľupa, J. Mareš, and O. Vyšata, "Remote physiological and GPS data processing in evaluation of physical activities," *Med. Biol. Eng. Comput.*, vol. 52, no. 4, pp. 301–308, Apr. 2014.
- [8] C. Hoffmann, "Effect of a facemask on heart rate, oxygen saturation, and rate of perceived exertion [auswirkung einer mund-nasen-bedeckung auf herzfrequenz, sauerstoffsättigung und subjektives belastungsempfinden]," *Deutsche Zeitschrift für Sportmedizin*, vol. 72, no. 7, pp. 359–364, 2021.
- [9] A. Curtiss, B. Rothrock, A. Bakar, N. Arora, J. Huang, Z. Enghardt, A. P. Empedrado, C. Wang, C. Ahmed, Y. Zhang, N. Alshurafa, and J. Hester, "FaceBit: Smart face masks platform," *Proc. ACM Interact., Mobile, Wearable Ubiquitous Technol.*, vol. 5, no. 4, p. 151:1–151:44, 2021.
- [10] G. Reychler, C. V. Straeten, A. Schalkwijk, and W. Poncin, "Effects of surgical and cloth facemasks during a submaximal exercise test in healthy adults," *Respiratory Med.*, vol. 186, Sep. 2021, Art. no. 106530.
- [11] E. T. Poon, C. Zheng, and S. H. Wong, "Effect of wearing surgical face masks during exercise: Does intensity matter?" *Frontiers Physiol.*, vol. 12, Jan. 2021, Art. no. 775750.
- [12] A. Scarano, F. Inchingolo, B. Rapone, F. Festa, S. R. Tari, and F. Lorusso, "Protective face masks: Effect on the oxygenation and heart rate status of oral surgeons during surgery," *Int. J. Environ. Res. Public Health*, vol. 18, no. 5, p. 2363, Feb. 2021.
- [13] S. Sanei, D. Jarchi, and A. G. Constantinides, *Body Sensor Networking, Design and Algorithms*. Hoboken, NJ, USA: Wiley, 2020.
- [14] D. Jarchi, J. Pope, T. K. M. Lee, L. Tamjidi, A. Mirzaei, and S. Sanei, "A review on accelerometry-based gait analysis and emerging clinical applications," *IEEE Rev. Biomed. Eng.*, vol. 11, pp. 177–194, 2018.
- [15] A. Procházka, H. Charvátová, S. Vaseghi, and O. Vyšata, "Machine learning in rehabilitation assessment for thermal and heart rate data processing," *IEEE Trans. Neural Syst. Rehabil. Eng.*, vol. 26, no. 6, pp. 1209–12141, Apr. 2018.
- [16] A. Procházka, O. Vyšata, H. Charvátová, and M. Vališ, "Motion symmetry evaluation using accelerometers and energy distribution," *Symmetry*, vol. 11, no. 7, p. 871, Jul. 2019.
- [17] H. Charvátová, A. Procházka, S. Vaseghi, O. Vyšata, and M. Vališ, "GPS-based analysis of physical activities using positioning and heart rate cycling data," *Signal, Image Video Process.*, vol. 11, no. 2, pp. 251–258, Feb. 2017.
- [18] A. Procházka, H. Charvátová, O. Vyšata, D. Jarchi, and S. Sanei, "Discrimination of cycling patterns using accelerometric data and deep learning techniques," *Neural Comput. Appl.*, vol. 33, no. 13, pp. 7603–7613, Jul. 2021.
- [19] A. Procházka, S. Vaseghi, H. Charvátová, O. Ľupa, and O. Vyšata, "Cycling segments multimodal analysis and classification using neural networks," *Appl. Sci.*, vol. 7, no. 6, p. 581, Jun. 2017.
- [20] E. Hostalkova, O. Vysata, and A. Prochazka, "Multi-dimensional biomedical image de-noising using Haar transform," in *Proc. 15th Int. Conf. Digit. Signal Process.*, Cardiff, U.K., Jul. 2007, pp. 175–179.
- [21] E. Jerhotová, J. Švihlík, and A. Procházka, *Biomedical Image Volumes Denoising via the Wavelet Transform*. Berlin, Germany: Springer, 2011, pp. 435–458.
- [22] B. Langari, S. Vaseghi, A. Prochazka, B. Vaziri, and F. T. Aria, "Edge-guided image gap interpolation using multi-scale transformation," *IEEE Trans. Image Process.*, vol. 25, no. 9, pp. 4394–4405, Sep. 2016.
- [23] K. Mutlu, J. E. Rabell, P. M. del Olmo, and S. Haesler, "IR thermography-based monitoring of respiration phase without image segmentation," *J. Neurosci. Methods*, vol. 301, pp. 1–8, May 2018.
- [24] A. Procházka, H. Charvátová, O. Vyšata, J. Kopal, and J. Chambers, "Breathing analysis using thermal and depth imaging camera video records," *Sensors*, vol. 17, no. 6, p. 1408, Jun. 2017.
- [25] A. Procházka, O. Vyšata, and V. Mařík, "Integrating the role of computational intelligence and digital signal processing in education: Emerging technologies and mathematical tools," *IEEE Signal Process. Mag.*, vol. 38, no. 3, pp. 154–162, Apr. 2021.
- [26] M. Fričl, "Video processing methods in thermographic analysis," M.S. thesis, Dept. Comput. Control Eng., Univ. Chem. Technol., Technicka, Prague, Czechia, Jun. 2022. [Online]. Available: <https://repozitar.vscht.cz/api/presentation/1.0/download/ae50e15c-0154-46f6-82aa-36b35e4387cc/>
- [27] R. Abedalmoniam and S. Fadul, "Oxygen level measurement techniques: Pulse oximetry," *SUST J. Syst.*, vol. 2, pp. 1–5, 2015.
- [28] B. Anupama and K. Ravishankar, "Working mechanism and utility of pulse oximeter," *Int. J. Sport, Exercise Health Res.*, vol. 2, no. 2, pp. 111–113, 2018.
- [29] J. L. Mildenhall, "The theory and application of pulse oximetry," *J. Paramedic Pract.*, vol. 1, no. 2, pp. 52–58, Nov. 2008.
- [30] L. Hooseok, H. Ko, and J. Lee, "Reflectance pulse oximetry: Practical issues and limitations," *Science Direct, Korean Inst. Commun. Inf. Sci.*, vol. 2, pp. 195–198, Dec. 2016.
- [31] T. Dünwald, R. Kienast, D. Niederseer, and M. Burtscher, "The use of pulse oximetry in the assessment of acclimatization to high altitude," *Sensors*, vol. 21, no. 4, p. 1263, Feb. 2021.
- [32] S. D. Din, A. Hickey, N. Hurwitz, J. C. Mathers, L. Rochester, and A. Godfrey, "Measuring gait with an accelerometer-based wearable: Influence of device location, testing protocol and age," *Physiol. Meas.*, vol. 37, no. 10, pp. 1785–1797, 2016.
- [33] O. Dostál, A. Procházka, O. Vyšata, O. Ľupa, P. Cejnar, and M. Vališ, "Recognition of motion patterns using accelerometers for ataxic gait assessment," *Neural Comput. Appl.*, vol. 33, no. 7, pp. 2207–2215, Apr. 2021.
- [34] A. Garcia-Garcia, S. Orts-Escolano, S. Oprea, V. Villena-Martinez, P. Martinez-Gonzalez, and J. Garcia-Rodriguez, "A survey on deep learning techniques for image and video semantic segmentation," *Appl. Soft Comput.*, vol. 70, pp. 41–65, Sep. 2018.
- [35] Y. Mo, Y. Wu, X. Yang, F. Liu, and Y. Liao, "Review the state-of-the-art technologies of semantic segmentation based on deep learning," *Neuro-computing*, vol. 493, pp. 626–646, Jul. 2022.
- [36] C. Sager, C. Janiesch, and P. Zschech, "A survey of image labelling for computer vision applications," *J. Bus. Anal.*, vol. 4, no. 2, pp. 91–110, Jul. 2021.
- [37] S. L. Shein, S. Whitticar, K. K. Mascho, E. Pace, R. Speicher, and K. Deakins, "The effects of wearing facemasks on oxygenation and ventilation at rest and during physical activity," *PLoS ONE*, vol. 16, no. 2, Feb. 2021, Art. no. e0247414.
- [38] R. P. Spang and K. Pieper, "The tiny effects of respiratory masks on physiological, subjective, and behavioral measures under mental load in a randomized controlled trial," *Sci. Rep.*, vol. 11, no. 1, p. 19601, Dec. 2021.
- [39] I. Wojtasz, S. Cofta, P. Czudaj, K. Jaracz, and R. Kaźmierski, "Effect of face masks on blood saturation, heart rate, and well-being indicators in health care providers working in specialized COVID-19 center," *Int. J. Environ. Res. Public Health*, vol. 19, no. 3, p. 1397, Jan. 2022.
- [40] J. T. Brooks and J. C. R. Butter, "Effectiveness of mask wearing to control community spread of SARS-CoV-2," *J. Amer. Med. Assoc.*, vol. 325, pp. 998–999, Mar. 2021.
- [41] S. Yang, C. Fang, X. Liu, Y. Liu, S. Huang, R. Wang, and F. Qi, "Surgical masks affect the peripheral oxygen saturation and respiratory rate of anesthesiologists," *Frontiers Med.*, vol. 9, Apr. 2022, Art. no. 844710.



HANA CHARVÁTOVÁ received the Ph.D. degree in chemistry and materials technology from the Technology of Macromolecular Substances, Faculty of Technology, TBU, Zlín, in 2007. She is currently associated with the Centre for Security, Information and Advanced Technologies (CEBIA–Tech), Faculty of Applied Informatics, TBU. Her research interests include modeling manufacturing processes of natural and synthetic polymers, analysis of thermal processes in build-

ing technology, studies of sensor system and wireless communication, signal processing for motion monitoring, and modeling of engineering and information systems. She is oriented towards computational and visualization methods in thermographics, spatial modeling, and engineering. She serves as a Reviewer for Springer, Elsevier, Wiley, Taylor & Francis, and MDPI journals.



ALEŠ PROCHÁZKA (Life Senior Member, IEEE) received the Ph.D. degree, in 1983. He was appointed as a Professor of technical cybernetics from Czech Technical University of Prague, in 2000. He is currently the Head of the Digital Signal and Image Processing Research Group, Department of Computing and Control Engineering, UCT, and the Czech Institute of Informatics, Robotics and Cybernetics, CTU, Prague. His research interests include mathematical methods of multidimensional data analysis, segmentation, feature extraction, classification, and modeling in biomedicine and engineering. He is a member of the IET and EURASIP. He has served as an Associate Editor for *Signal, Image and Video Processing* journal (Springer). He is a reviewer for different IEEE TRANSACTIONS, Springer, Elsevier, and MDPI journals.



MATĚJ FRIČL received the M.Sc. degree in sensors and technical cybernetics in chemistry from the University of Chemistry and Technology in Prague, Czech Republic, in 2022. He is currently a member of the Digital Signal and Image Processing Research Group, Department of Computing and Control Engineering. His research interests include information engineering, programming methods, visualization tools, computational methods of multidimensional data analysis, feature extraction, machine learning, and classification. Applications of his research are devoted to biomedicine, neurology, and physiological data processing.



OLDŘICH VYŠATA (Member, IEEE) received the M.D. and Ph.D. degrees in technical cybernetics from the University of Chemistry and Technology in Prague (UCT Prague), Czech Republic, in 1985 and 2011, respectively. He is currently a member of the Digital Signal and Image Processing Research Group, Department of Computing and Control Engineering, UCT Prague, the European Neurological Society, the Czech Society of Clinical Neurophysiology, the Czech League Against Epilepsy, and the Czech Medical Association of J. E. Purkyně. He is also associated with the Neurological Department, University Hospital of the Charles University at Hradec Králové, Czech Republic. He is oriented towards computational medicine, analysis of motion disorders, and machine learning. He serves as a reviewer for different Springer, Elsevier, and MDPI journals.

• • •